Infectious Disease Modelling 9 (2024) 373–386

Contents lists available at ScienceDirect

Infectious Disease Modelling

journal homepage: www.keaipublishing.com/idm

The non-stationary and spatially varying associations between hand, foot and mouth disease and multiple environmental factors: A Bayesian spatiotemporal mapping model study

Li Shen [a,1], Minghao Sun [a,1], Mengna Wei [a,1], Qingwu Hu [a], Yao Bai [b,***], Zhongjun Shao [c,**], Kun Liu [c,*]

[a] *School of Remote Sensing and Information Engineering, Wuhan University, Wuhan, Hubei Province, China*
[b] *Department of Infection Disease Control and Prevention, Xi'an Center for Disease Control and Prevention, Xi'an, Shaanxi, China*
[c] *Department of Epidemiology, Ministry of Education Key Lab of Hazard Assessment and Control in Special Operational Environment, School of Public Health, Air Force Medical University, Xi'an, Shaanxi Province, China*

A R T I C L E I N F O

Article history:
Received 29 December 2023
Received in revised form 29 January 2024
Accepted 4 February 2024
Available online 10 February 2024
Handling Editor: Dr Yijun Lou

Keywords:
Hand, foot, and mouth disease (HFMD)
Environmental factors
Bayesian spatiotemporal mapping model
Non-stationary effects
Spatially varying effects

A B S T R A C T

The transmission and prevalence of Hand, Foot and Mouth Disease (HFMD) are affected by a variety of natural and socio-economic environmental factors. This study aims to quantitatively investigate the non-stationary and spatially varying associations between various environmental factors and HFMD risk. We collected HFMD surveillance cases and a series of relevant environmental data from 2013 to 2021 in Xi'an, Northwest China. By controlling the spatial and temporal mixture effects of HFMD, we constructed a Bayesian spatiotemporal mapping model and characterized the impacts of different driving factors into global linear, non-stationary and spatially varying effects. The results showed that the impact of meteorological conditions on HFMD risk varies in both type and magnitude above certain thresholds (temperature: 30 °C, precipitation: 70 mm, solar radiation: 13000 kJ/m^2, pressure: 945 hPa, humidity: 69%). Air pollutants ($PM_{2.5}$, PM_{10}, NO_2) showed an inverted U-shaped relationship with the risk of HFMD, while other air pollutants (O_3, SO_2) showed nonlinear fluctuations. Moreover, the driving effect of increasing temperature on HFMD was significant in the 3-year period, while the inhibitory effect of increasing precipitation appeared evident in the 5-year period. In addition, the proportion of urban/suburban/rural area had a strong influence on HFMD, indicating that the incidence of HFMD firstly increased and then decreased during the rapid urbanization process. The influence of population density on HFMD was not only limited by spatial location, but also varied between high and low intervals. Higher road density inhibited the risk of HFMD, but higher night light index promoted the occurrence of HFMD. Our findings further demonstrated that both ecological and socioeconomic environmental factors can pose multiple driving effects on increasing the spatiotemporal risk of HFMD, which is of great significance for effectively responding to the changes in HFMD epidemic outbreaks.

* Corresponding author.
** Corresponding author.
*** Corresponding author.
E-mail addresses: baiyaocdc@163.com (Y. Bai), 13759981783@163.com (Z. Shao), liukun5959@qq.com (K. Liu).
Peer review under responsibility of KeAi Communications Co., Ltd.
[1] These authors have contributed equally to this work and share first authorship.

https://doi.org/10.1016/j.idm.2024.02.005

1. Introduction

Hand, foot, and mouth disease (HFMD) is an intestinal infectious disease caused by enterovirus, which commonly causes infection among children under 5 years old. The serotypes of enteroviruses detected in HFMD cases mainly include Enterovirus A71 (EV-A71), Coxsackievirus A16 (CV-A16) and Coxsackievirus A6 (CV-A6) in recent years (Esposito & Principi, 2018). The virus has been found in the excreta, herpes fluid, and respiratory secretions of confirmed HFMD cases and those with latent infection, and further spread to other susceptible people through fecal-oral transmission, droplets, and contact with contaminated objects. The incubation period of HFMD generally experiences 2–10 days and the incidence of HFMD has obvious seasonal characteristics (Simonart, Lam Hoai, & De Maertelaer, 2022). Severe epidemics and outbreaks of HFMD in the Western Pacific region and East Asian countries have resulted in a heavy health and economic burden. In China, more than 20 million cases of HFMD have been reported since it was first included in the monitoring and management system in 2008, and its annual incidence ranks in the forefront of various infectious diseases (Hong et al., 2022).

The transmission mechanism of HFMD is multiplex, and its epidemic dynamics is not only directly affected by enterovirus activity and human immunity, but also closely associated to various environmental factors. A deeper understanding of the association between HFMD and those relevant factors will effectively help predict the incidence to prevent further transmission (Zhu et al., 2023). The survival and reproduction ability of the enterovirus of HFMD is quite sensitive to meteorological factors, especially with temperature and humidity showing a stronger influence (Tian, Liang, et al., 2018). Human behavior patterns change in different meteorological conditions, which can accordingly affect the probability of contact with the enterovirus, such as less outdoor activities in cold and rainy days evidently reducing the virus transmission (Wang et al., 2019). Taking further account of human-caused air pollution, both positive (e.g. SO_2 and NO_2) and negative (e.g. O_3 and PM_{10}) effects on the risk of HFMD have been also observed (He et al., 2020). In addition, sewage during flood season and vegetation cover can also modify the enterovirus transmission efficiency (Du et al., 2018; Hu, Jiang, & Ni, 2018), suggesting that the importance of surface environment cannot be ignored in epidemiology of HFMD. Moreover, the transformation of socio-economic environment usually leads to the inertial flow and aggregation of the population, which will facilitate the contact between individuals, and a higher incidence of HFMD is also taken for granted (Gou et al., 2017). However, at the same time, this process will also improve the local public health condition and optimize the allocation of medical resources. Therefore, in some cases, the risk of HFMD appears relatively low in areas with convenient transportation and commercial prosperity, which can be observed in the distribution patterns of other infectious diseases (Lei et al., 2023; Li, Zhu, et al., 2022). In terms of human intervention, specific vaccination is the most effective means to curb the spread of HFMD. Since the launch of EV-A71 vaccination in 2016, the proportion of severe cases of HFMD in China has dropped significantly, and the proportion of young cases has also decreased (Hong et al., 2022). Nevertheless, most previous researches are limited to not considering the nonlinear relationship between ecological environmental factors and HFMD risk, and especially the impact of interannual fluctuations of meteorological conditions remains speculative. What's more, the response of HFMD risk to socio-economic factors in different regions and stages of development has not been fully understood.

In order to more accurately capture the relationship between HFMD and potential environmental factors, in this study we developed a comprehensive Bayesian spatiotemporal mapping model to conduct a quantitative analysis. We incorporated the historical surveilled HFMD and multiple relevant environmental factors into this proposed Bayesian spatiotemporal model, and came up with specific interpretation according to different effect types.

2. Materials and methods

2.1. Study area

This retrospective epidemiology research was carried out in Xi'an (107°40′-109°49′ E, 33°42′-34°45′ N), the capital city of Shaanxi Province and the largest regional central city in Northwest China. The city of Xi'an consists of 11 administrative districts and two counties covering a total area of 10,752 km^2 with a permanent population of 12.95 million in 2020 (http://tjj.xa.gov.cn/). Benefited from both tourism advantages and economic primacy, Xi'an has experienced frequent population movements and rapid urbanization in recent years. Meanwhile, the urgency of HFMD in Xi'an has gradually become prominent and a total of 181,358 cases of HFMD were reported from 2009 to 2018 (Guo et al., 2020). The high-incidence period of HFMD in Xi'an City includes April-July and October-November, and its spatial aggregation characteristics are more noticeable than other areas in the province (Zhu et al., 2021).

2.2. Data collection and process

We obtained the reported 2013–2012 historical HFMD data for Xi'an from the Center for Disease Control and Prevention of Xi'an, Shaanxi Province. Raw case data were stored in tabular form and individual attributes included gender, age, address, date of onset, etc. Firstly, we integrated the information from initial diagnosis and excluded some records with symptoms similar to those of HFMD. Secondly, we removed records beyond our study period and region according to the resident locations of HFMD cases and the exact date of onset. Finally, we utilized geocoding technology to convert the address text into spatial points with latitude and longitude and aggregated them down to the town-level area. After data cleansing and screening process described above, we obtained a total of 172,894 HFMD cases in Xi'an from January 1, 2013 to December 31, 2021.

Data of environmental factors can be classified into two major categories, natural environment and socio-economic environment. Meteorological data was obtained from the ERA5-land dataset of Copernicus Climate Change Service (Muñoz, 2019), including temperature (°C), total precipitation (mm), dewpoint temperature (°C), surface pressure (hPa), total evaporation (mm), surface net solar radiation (kJ/m^2), and east-west and north-south wind speed (m/s). Relative humidity (%) was calculated from temperature and dewpoint temperature. Atmospheric particles and air pollution data was obtained from the ChinaHighAirPollutants (CHAP) dataset (Wei et al., 2021, 2023), including $PM_{2.5}$, PM_{10}, O_3, SO_2 and NO_2. Population density was collected from the Individual countries 2000–2020 UN adjusted dataset of the WorldPop platform (WorldPop, 2022). Nightlight data was acquired from A Prolonged Artificial Nighttime-light Dataset of China (PANDA) dataset (Zhang et al., 2021) and normalized to the interval [0, 1]. Land cover data was retrieved from land cover products from 1985 to 2020 of China (Yang & Huang, 2021) and we combined the distribution of impervious surfaces and population density to extract the range of urban, suburban and rural areas in Xi'an. We derived road data from the OpenStreetMap (OSM) dataset, and obtained points of interest (POIs) data from the Shaanxi Province Public Data Open Platform (Shaanxi Provincial Public Data Platform, 2022), including kindergartens, primary schools, dining establishments and medical institutions. Altitude data was acquired from the ASTER GDEM dataset (Geospatial Data Cloud, 2009) and map data of Xi'an was downloaded from National Catalogue Service for Geographic Information of China.

The guiding principle in data cleaning process is to preserve the characteristic information of the original data as much as possible. First two steps mainly involved excluding those confirmed non-HFMD cases after examining the residential addresses outside Xi'an or disease onset time beyond the study period. Next, we converted the textual data into spatial data, with partially detailed addresses uniformly categorized into township centers. This categorization ensures results unaffected when analyzing at the township level.

2.3. Statistical analysis

In this study, based on the Bayesian hierarchical model (BHM) framework, we developed a Bayesian spatiotemporal mapping model by incorporating the effects of different factors (Formula 1). Y_{it} denotes the number of HFMD cases for town-level area i in month t, following a Poisson distribution. E_{it} represents the expected number of HFMD cases, calculated from the overall incidence in Xi'an. We further modeled the relative risk (RR) θ_{it} as the additive structure consisting of spatial, temporal effects and covariates. u_i means the structural spatial effect, following a conditional autoregressive (CAR) prior. λ_t is the structural temporal effect, grouped by month and subject to a first-order autoregressive (AR1) prior. The description of Conditional Autoregressive (CAR) prior is given by Formula (2):

$$Y_{it} \sim Poisson(E_{it}\theta_{it})$$

$$log(\theta_{it}) = \alpha + u_i + v_i + \lambda_t + \gamma_t + \xi_{it} +$$

$$\sum_{p=1}^{p} x_{p,ij}^{land} + \sum_{m=1}^{m} f\left(x_{m,ij}^{meteor-pollute}\right) + \sum_{n=1}^{n} f\left(\beta_{n,i} x_{n,ij}^{socio-eco}\right) \tag{1}$$

$$u_i | u_j, i \neq j, \sim N\left(\frac{\alpha}{m_i}\sum_{i \sim j} u_j, \frac{1}{m_i \tau}\right) \tag{2}$$

Where m_i denotes the total number of adjacent regions for region i, $i \sim j$ indicates that regions i and j are adjacent, and τ is the precision hyperparameter. The mean of the normal distribution is determined by the spatial effects of adjacent regions, with this study setting the spatial smoothing parameter α to 1 and using a first-order Queen spatial adjacency matrix to define adjacency relationships.

We set the prior of the nonstructural spatial effect v_i and temporal effect γ_t to a Gaussian distribution, and α denotes the fixed intercept. The model incorporates three functions: linear regression, smoothing functions, and Spatially Varying Coefficient (SVC), to include influencing factors. Since the relationship between socioeconomic factors and the risk of HFMD varies across different spatial locations, choosing spatial variation coefficients can better reduce the spatial errors when it comes to capture this heterogeneous phenomenon.

The relationship between different land cover areas (cropland, forest, and impervious area) and land use areas (urban, suburban, and rural) in Xi'an and the incidence rate of HFMD needs to be aggregated differently at the township level. Therefore, a global linear regression approach is used for modeling. Meteorological factors and air pollutants $x^{meteor\text{-}pollute}$ are nonlinearly correlated with the incidence rate of HFMD, and thus, smoothing functions are employed for modeling. Spline functions are a common choice for smoothing, effectively achieving local smoothing through segmented fitting. However, penalties are applied to the nodes and coefficients to avoid excessive complexity, as shown in Formula (3). The coefficient b is used for penalty, and in the Bayesian modeling framework, applying penalties can be viewed as setting a first-order random walk prior on the covariate coefficients, as shown in Formula (4), where k represents the segmented nodes of the covariates, and the current node's covariate coefficient value is generated by adding Gaussian noise to the value of the previous node. In this study, segmented nodes of covariates were generated using equidistant quantiles, and the original data were transformed into segmented data. The relationship between socio-economic factors $x^{socio\text{-}eco}$ and the incidence rate of HFMD varies at different spatial locations. Therefore, modeling is based on spatially varying coefficients, which essentially involves a random slope model. In the Bayesian framework, random slopes, also known as local regression coefficients, can be assigned CAR priors, where the distribution of coefficient values is correlated with those of neighboring regions. Similar to structured spatial effects, spatial weights for the SVC model were established using a first-order queen adjacency matrix in this study. The posterior marginal variances of the different components were derived to compare the contribution to the total variability of the risk. The Bayesian spatiotemporal mapping model established in this study was implemented using the R-INLA v.21.02.23 package (www.r-inla.org), within the R software environment (version 4.0.5).

$$min \sum_{i=1}^{n} (y_i - f(x_i))^2 + \lambda \left(\sum_{k=1}^{p} b_k^2 \right) \tag{3}$$

$$f(\kappa_{i+1}) - f(\kappa_i) \sim N(0, \tau), i = 1, ..., K-1 \tag{4}$$

3. Results

3.1. Linear effects of surface environmental factors

Surface environmental factors primarily consist of topography, land cover and land use, which pose more significant impacts on HFMD risk from an overall research perspective. Considering the Qinling Mountains and Weihe Plains with great differences in elevation, the influence of altitude on the incidence of HFMD in Xi'an cannot be ignored. The results of the posterior regression coefficient in Table 1 show that for every 1 m increase in the regional average altitude, the relative risk of HFMD decreases by 0.02%. The inhibitory effect of increased altitude on the incidence of HFMD can be explained by that the sparse population in mountainous areas leads to less human-to-human transmission of enteroviruses. According to the spatial distribution of HFMD cases in Xi'an, as illustrated in Fig. 1, more than 90% of the cases lived in areas below an altitude of 700 m. However, the spatial distribution of HFMD cases living in areas above 700 m demonstrates less but significant clustering characteristics. Clustering area 1 is located in the higher mountainous valleys, and clustering area 2 is located in the lower plateau forms surrounded by plains. In addition, as shown in Fig. 1(b), the proportion of HFMD cases above an altitude of 1000 m except for 2020 has decreased year by year since 2016.

Among the various types of land cover in Xi'an, cropland, forest and impervious area are more closely related to HFMD risk due to their higher proportions. The mean value of the posterior regression coefficient of cropland and forest is negative,

Table 1
The posterior distribution and relative risk of global linear coefficients between impact factors and HFMD risk in Xi'an, 2013–2021. The factors in the table were incorporated as linear terms into the Bayesian spatiotemporal mapping model, where the temporal resolution is 1 year except for average altitude.

Factors		Posterior coefficient			RR [c]
		Mean	S.D. [a]	95% CI [b]	
Topography	Average altitude (m)	−0.000186	0.000147	(-0.000474, 0.000102)	0.999814
Land cover	Cropland (A.P.) [d]	−0.006913	0.006059	(-0.018808, 0.004975)	0.993111
	Forest (A.P.)	−0.003851	0.006113	(-0.015851, 0.008141)	0.996157
	Impervious area (A.P.)	0.003456	0.007351	(-0.010977, 0.017877)	1.003462
Land use	Urban area (A.P.)	−0.012857	0.006540	(-0.025696, −0.000026)	0.987225
	Suburban area (A.P.)	0.017945	0.007124	(0.003952, 0.031917)	1.018107
	Rural area (A.P.)	−0.007710	0.007220	(-0.021886, 0.006454)	0.992320

[a] S.D.: standard deviation.
[b] 95%CI: 95% credible interval.
[c] RR: relative risk.
[d] A.P.: area proportion.

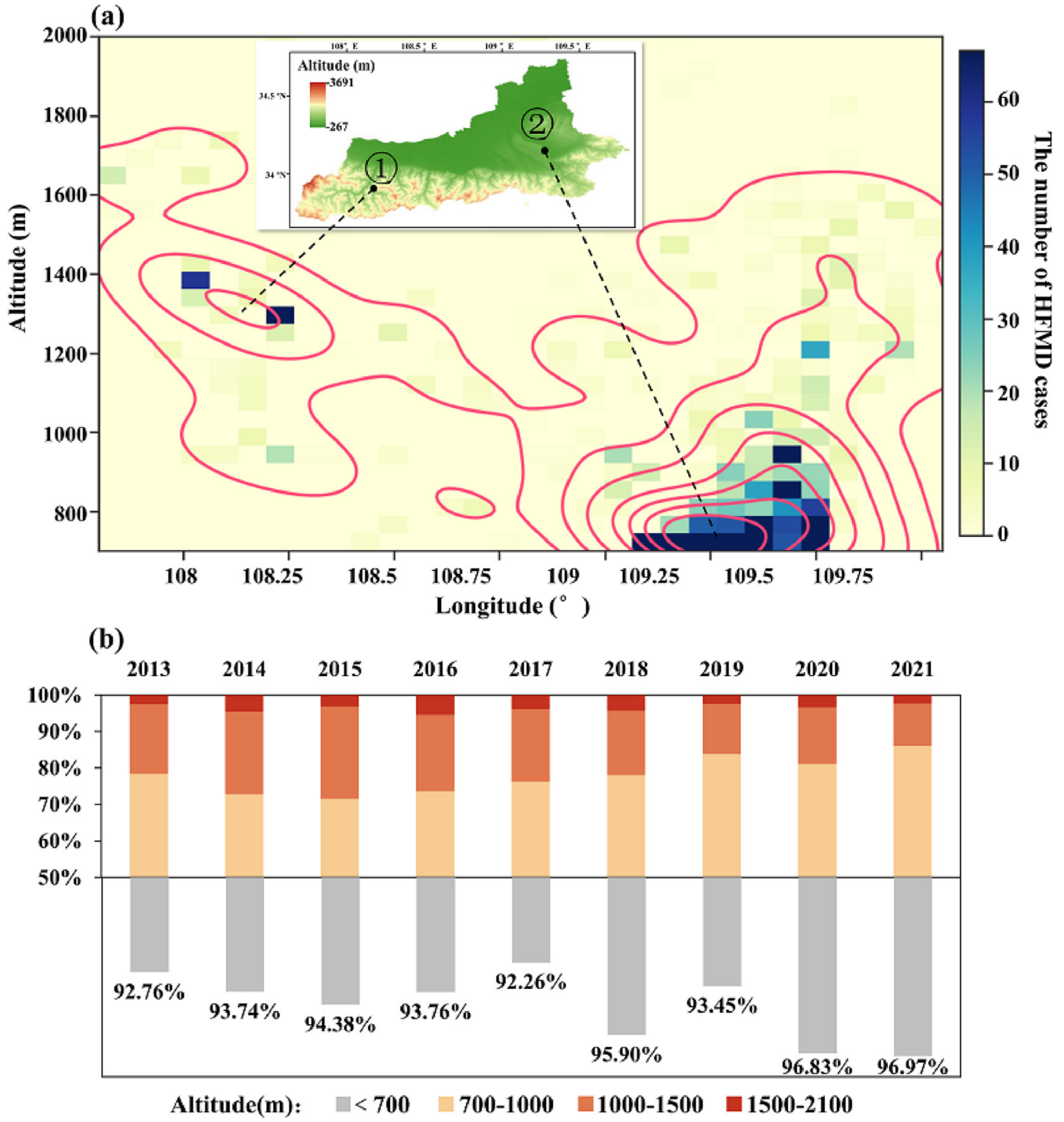

Fig. 1. The altitude distribution of habitations of HFMD cases in Xi'an, 2023-2021. (a) The spatial distribution of HFMD cases at altitudes above 700m. Heatmaps and 2-D kernel density curves indicate the local number of HFMD cases. (b) The proportion of HFMD cases in different altitude intervals. The proportion of HFMD cases below 700 m is shown in gray columns, and the proportion above 700m is shown by partitions.

while that of impervious surface is positive. When the proportion of cropland and forest increases by 1%, the relative risk of HFMD decreases by 0.69% and 0.38%, respectively. In contrast, every 1% increase in the proportion of impervious area results in a 0.35% increase in the relative risk of HFMD. Among the land use types, the risk of HFMD is only positively correlated with the proportion of suburban area, and for every 1% increase, the relative risk of HFMD grows by 1.81%. When the proportion of urban and rural area increases by 1%, the relative risk of HFMD dropped by 1.28% and 0.77%, respectively. In terms of inter-category comparison, the change in the proportion of cropland in land cover has a greater impact on HFMD risk, while for land uses the change in the proportion of suburban area has the most significant influence.

3.2. Non-stationary effects of meteorological factors and air pollutants

The risk of HFMD responds sensitively to the changes in meteorological conditions, among which temperature is the most notable factor. As shown in Fig. 2, the RR value gradually grows from lower than 1 to higher than 1 as the temperature increases, indicating that the relative risk of HFMD is higher than the overall risk (RR > 1) when it comes to higher temperature. However, from Fig. 2 (b) we can find that the continual growth of RR value weakens when the temperature exceeds 30 °C, revealing that extremely high temperature can inhibit the incidence of HFMD to a certain extent. The temperature in Xi'an is

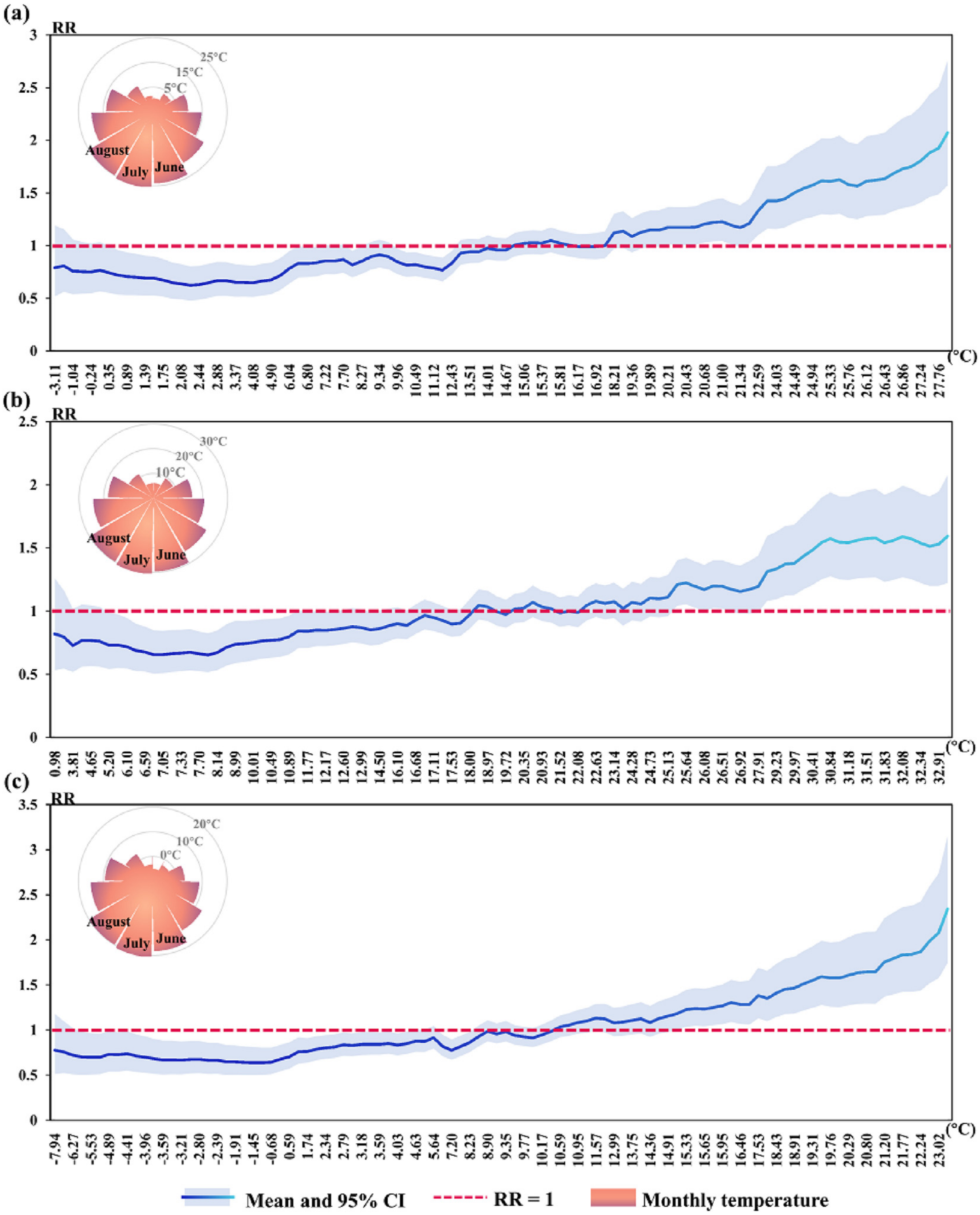

Fig. 2. The monthly value and posterior RR between (a) average temperature, (b) maximum temperature and (c) minimum temperature and HFMD risk in Xi'an, 2013–2021. The RR values were exponentially converted from the posterior distribution of coefficients at different temperatures, and the monthly temperature is the mean value over the study period.

relatively high from June to August every year, which overlaps with the high-incidence season of HFMD (April-July). Another previously overlooked meteorological factor is wind, as indicated in Supplementary Fig. S1 of Appendix A, changes in the relative risk of HFMD caused by east-west winds is more pronounced than that caused by north-south winds. Especially when the speed of east-west wind rises, the RR value continues to grow to the peak, confirming that the enterovirus spreads faster under this wind condition. With respect to other meteorological factors, as shown in Supplementary Fig. S2, the relationship between precipitation and surface net solar radiation and the relative risk of HFMD appears similar, while factors of surface pressure and relative humidity have comparable impact on HFMD incidence. When precipitation and surface net solar radiation exceed their respective thresholds (70 mm; 13000 kJ/m^2), the relative risk of HFMD decreases first and then increases significantly. Conversely, surface pressure and relative humidity are only below certain thresholds (945 hPa; 69%) where the relative risk of HFMD is higher than the overall risk. Besides, the stable RR value around 1 of evaporation shows that it has no significant relationship with HFMD, which can be seen from Fig. S2 (e).

Temperature and precipitation are the two most fluctuating meteorological factors, so the impact of interannual changes on the risk of HFMD was further analyzed for them. As shown in Fig. 3 (b) and (c), the 3-year and 5-year temperature changes have almost similar effects on HFMD, that is, when the increase of temperature is large, the relative risk of HFMD rises significantly. The effects of changes in precipitation between different years on the risk of HFMD is basically in the same pattern, as indicated in Fig. 3 (d), (e) and (f). The precipitation decrease for the 1-year, 3-year and 5-year period all promotes the relative risk of HFMD, while the increase of precipitation only causes a large decline in the relative risk for the 5-year period. In addition, the distribution of the posterior mean in Fig. 3 (g) and (h) reveals that the relative risk of HFMD changes more obviously under the 3-year temperature fluctuation, but it is more significant under the 1-year and 5-year precipitation fluctuations.

In terms of the association between air pollutants and HFMD risk, there appears an inverted U-shaped which mainly involves particulate matter and NO_2. It can be seen from Fig. 4 (a), (b) and (e) that when the pollutant monitoring value is in the middle range, the relative risk of HFMD is higher than the overall risk, while when the monitoring value is too high or too low, the relative risk is correspondingly inhibited. Different from the above pollutants, when the monitoring value of O_3 increases, the RR value also gradually rises, as shown in Fig. 4 (c), indicating that high concentration of O_3 will promote the relative risk of HFMD. Finally, SO_2 also drives HFMD risk at higher concentrations, as shown in Fig. 4 (d), but the relative risk drops sharply near the highest concentration. This interesting relationship is more likely to be associated with the seasonal variation of SO_2, because the dispersion of its monitoring values in different areas of Xi'an is much smaller than that of other pollutants (see Supplementary Fig. S3).

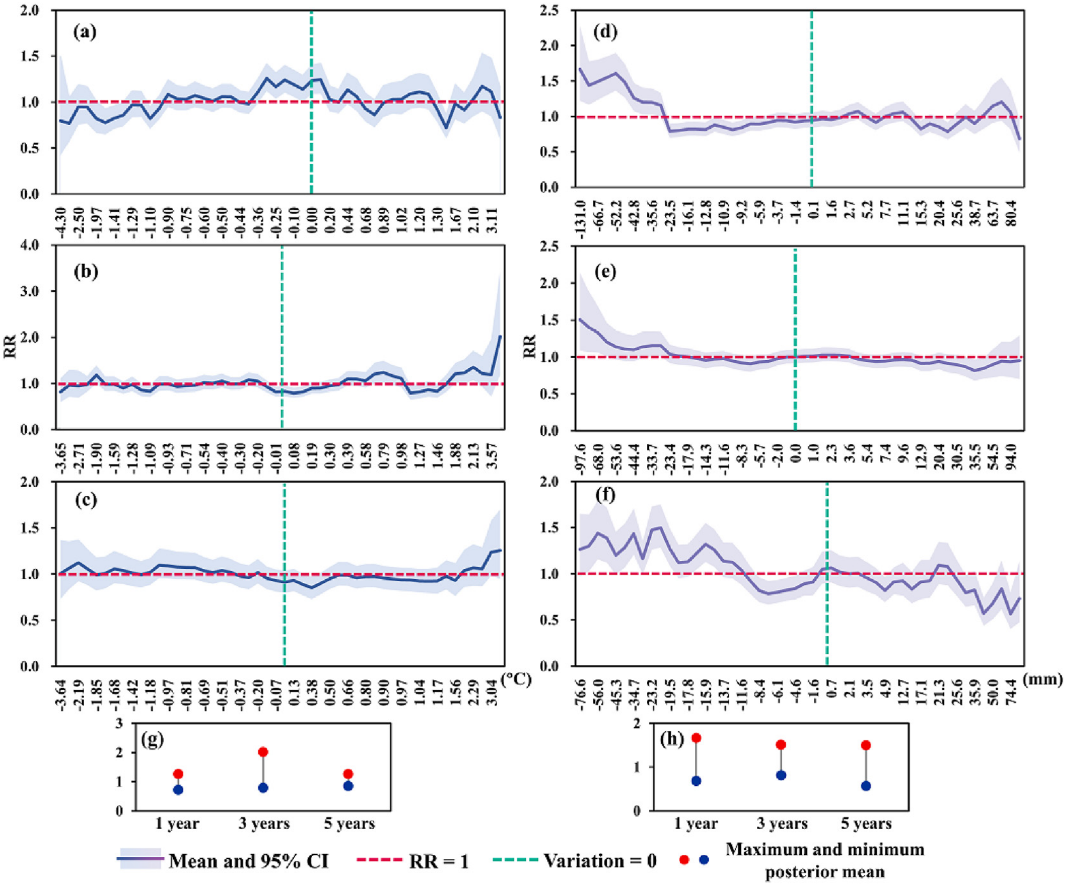

Fig. 3. The posterior RR between interannual fluctuations in temperature and precipitation and HFMD risk in Xi'an, 2013–2021. (a)-(c) Results for temperature differences between 1 year, 3 years, and 5 years. (d)-(f) Results for precipitation differences between 1 year, 3 years, and 5 years. (g)-(h) The maximum and minimum posterior mean RR of temperature and precipitation fluctuations. The difference between temperature/precipitation was calculated by moving over different length Windows (1, 3, 5 years) during the study period. The maximum and minimum posterior RR shows the magnitude of temperature/precipitation fluctuations over a certain length of time.

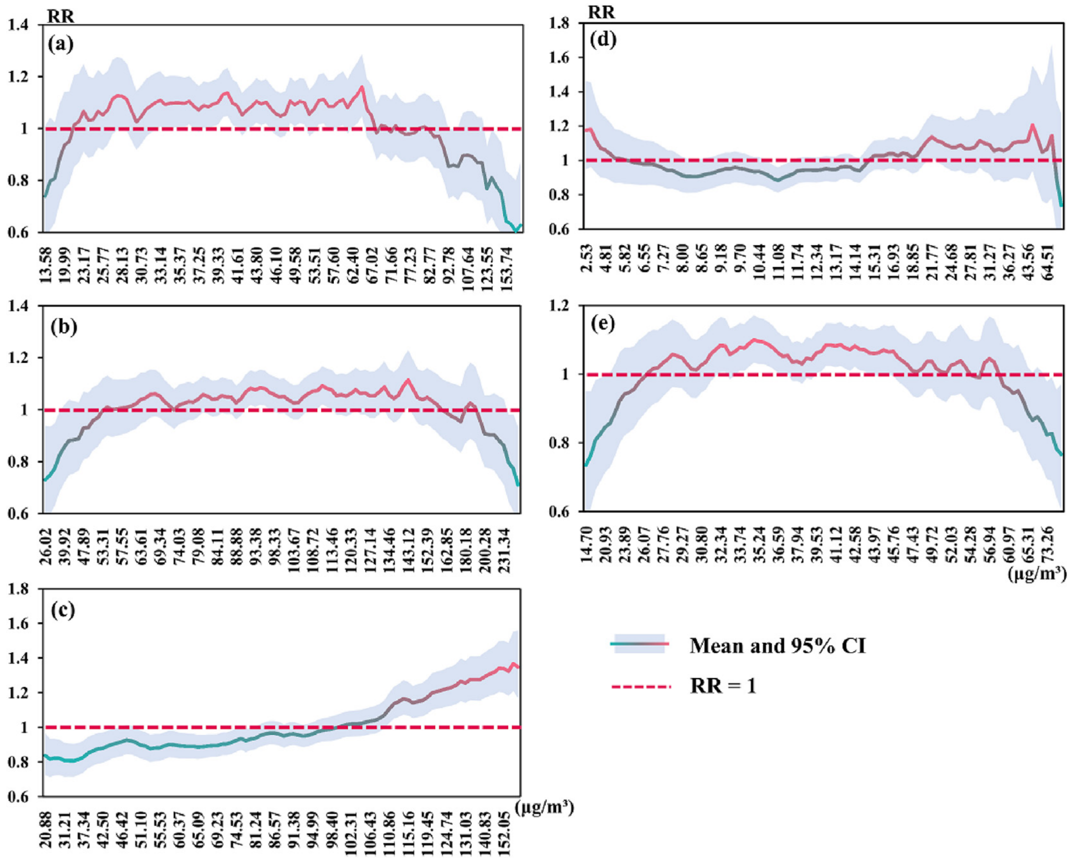

Fig. 4. The posterior RR between atmospheric particles and air pollutants and HFMD risk in Xi'an, 2013–2021. (a)-(b) Results for $PM_{2.5}$ and PM_{10}. (c)-(e) Results for O_3, SO_2 and NO_2. The unit of measurement of atmospheric particles matter and air pollutants was unified to micrograms per cubic meter, and the interval number in the process of converting continuous data into classified data is 100.

3.3. Spatially varying effects of socio-economic environmental factors

In different stages of urbanization, the growth rate of population tends to change, so this study compared the impact of population density on HFMD risk before and after median segmentation. When not segmented, as shown in Fig. 5 (a), the areas where population density is positively correlated with the relative risk of HFMD (RR > 1) mainly include the northeast and southwest of the core urban area, and some westernmost areas. The areas where population density is negatively correlated with HFMD risk are mostly distributed in the eastern and central rural areas. After population density segmentation, as shown in Fig. 5 (b) and (c), the population density in the western region and the relative risk of HFMD became positively correlated in the low-density stage, while the correlation in the eastern region was mostly negative. In the high-density stage, similar to the unsegmented situation, the areas with a positive correlation between population density and HFMD risk are concentrated in the northeast of Xi'an. Moreover, before and after segmentation, the population density of some communities in the core urban area has always been negatively correlated with the relative risk of HFMD.

Road density and nightlight can be used as effective indicators to measure the regional economic level for analyzing the impact of urbanization on HFMD. From Fig. 6 we can see that the road density is mainly positively correlated with the relative risk of HFMD in the northeast and west of Xi'an, while the normalized nightlight is positively correlated with HFMD risk primarily in the east and north. In particular, when the local area value is high, as demonstrated in the scatter plot of Fig. 6, the road density is negatively correlated with the relative risk of HFMD, while the nighttime light is more positively correlated. In terms of public facilities, we analyzed the impact of the number of different types of POIs on HFMD risk. The areas where the number of POIs is positively correlated with the relative risk of HFMD are mostly distributed around the core urban area of Xi'an, as shown in Supplementary Fig. S4. Limited by the lower economic level, the number of POIs in the western region is mostly negatively correlated with the relative risk of HFMD. Besides, the proportion of posterior marginal variances shown in Fig. S4 (e) indicates that the number of primary schools and kindergartens has a much greater impact on HFMD risk than the dining establishments and medical institutions.

Finally, the contribution of different components in Bayesian models to the variation in HFMD risk was compared according to the proportion of posterior marginal variances. As shown in Fig. 7, when the environmental factors were not

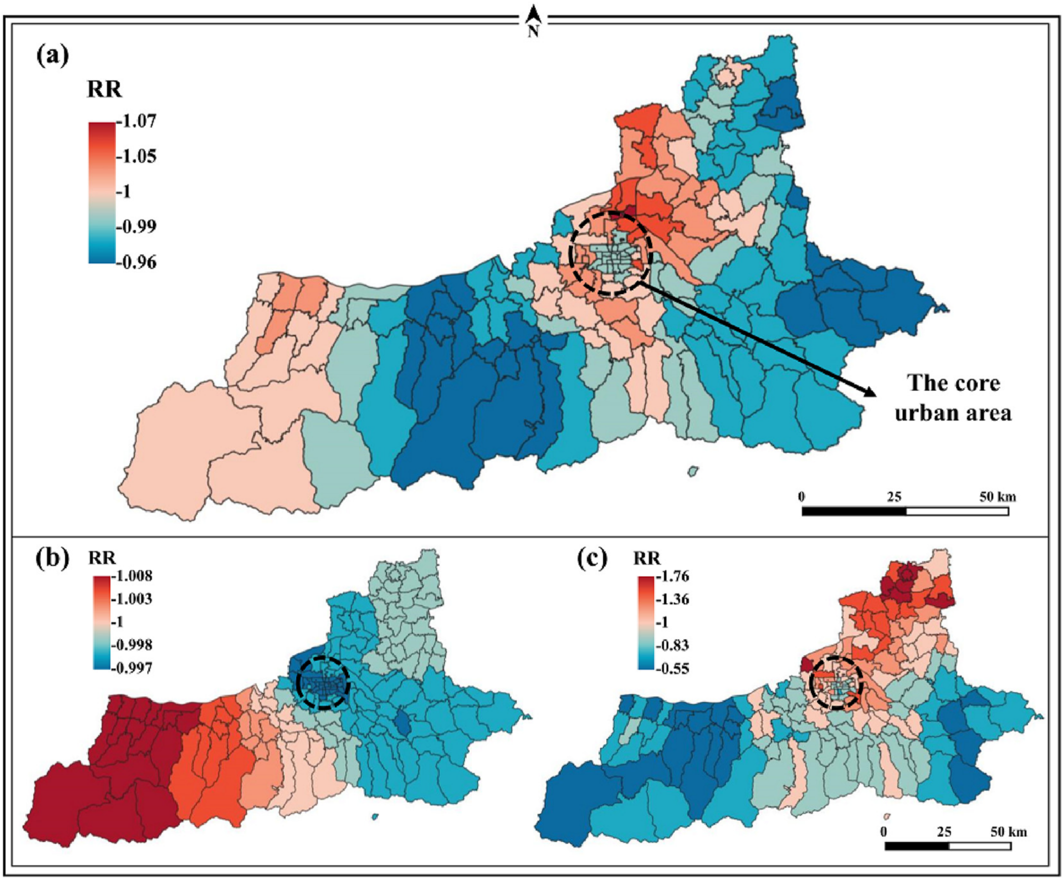

Fig. 5. The spatial distribution of posterior RR between population density and HFMD risk in Xi'an, 2013–2021. (a) Results for the entire population density interval. (b) Results for the low population density interval. (c) Results for the high population density interval. We used a B-spline function with one node to segment the population density, and the spatial and temporal resolutions before and after the segmentation were consistent.

included, the structural temporal effect can explain 76.56% of the variability in the HFMD risk. After incorporating non-stationary effects caused by natural environmental factors, only the proportion of structural temporal effect declined significantly, while after incorporating spatially varying effects caused by socio-economic factors, the proportions of temporal and spatial effects both decreased. This result suggests that the inclusion of environmental factors can help link the generalized spatiotemporal risk of HFMD to the specific impacts of different factors, as well as explain the spatiotemporal effects.

4. Discussion

4.1. Principal results and comparison with prior work

As an interdisciplinary research, this study integrated multi-source data into a Bayesian spatiotemporal model to comprehensively investigate the impacts of various environmental factors posed on HFMD risk. Results indicate that the relationship between the relative risk of HFMD and potential factors is not only restricted by the local natural environment, but also by the obvious fluctuations existing in human activities. Altitude was firstly analyzed due to its apparent variation within the study area, which leads to a result consistent with the experience that most HFMD cases reside in densely populated plains (Zhang, Xu, & Xiao, 2020). In addition, we detected a clustered distribution of HFMD cases in high-altitude areas, but the proportion of cases above 1000 m decreased significantly after 2016, which may be related to the relocation and poverty alleviation implemented by Xi'an government (Xi'an Municipal People's Government, 2022). Although living at lower altitude areas does not mean that the population is less likely to be exposed to enteroviruses, HFMD patients can receive medical attention more promptly after symptoms appearing. Analysis of other surface environmental factors, including land cover and land use, suggests that built-up areas expansion and encroachment on vegetated areas act as key drivers to increase the risk of HFMD. Moreover, our results further confirmed that the relative risk of HFMD increased during the transition from rural areas to suburban areas, while then decreased during the transition from suburban areas to urban areas. This finding is consistent to previous studies that identified the incidence thresholds for infectious diseases during urbanization (Shen, Sun,

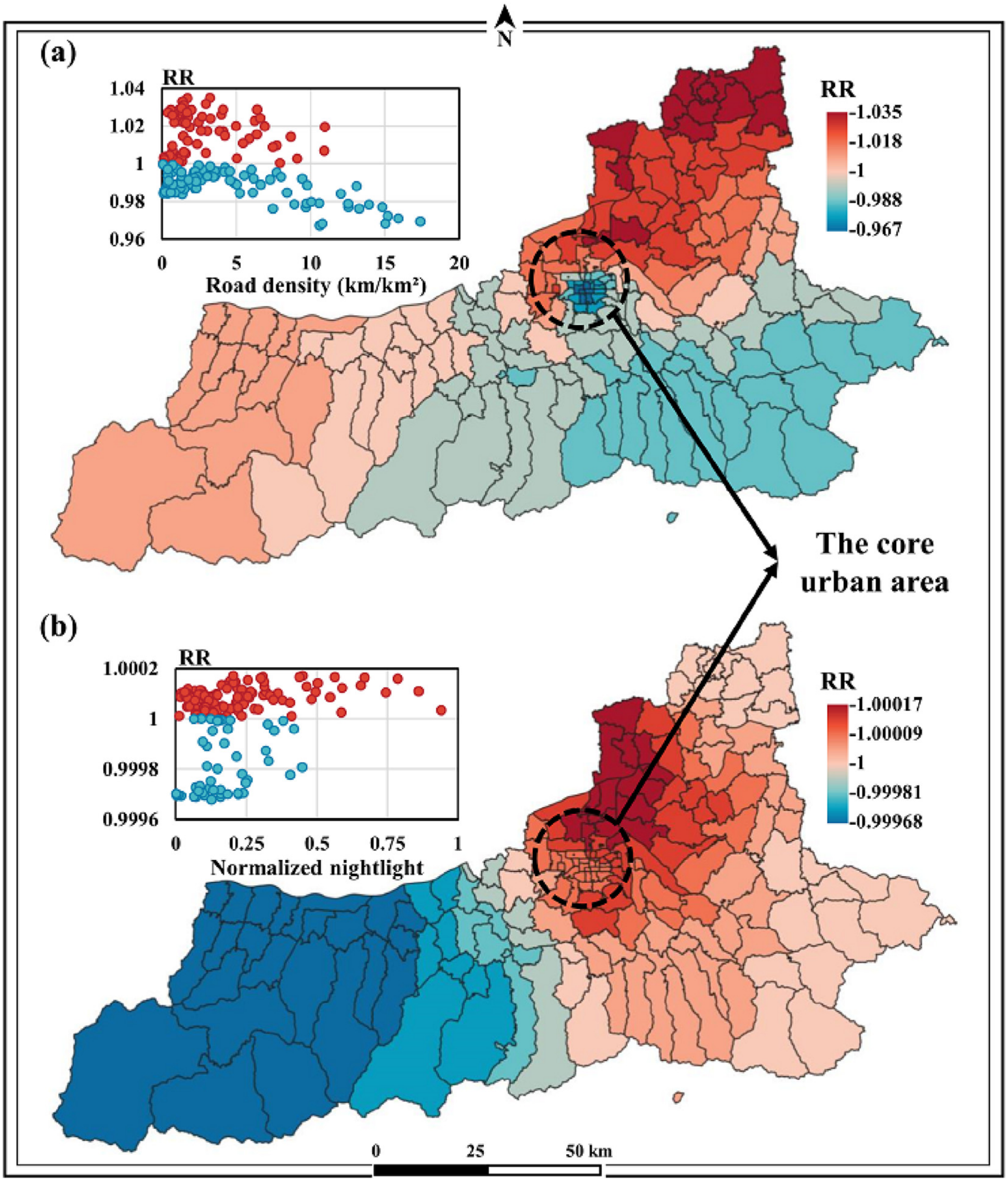

Fig. 6. The spatial distribution of posterior RR between (a) road density and (b) normalized nightlight and HFMD risk in Xi'an, 2013–2021. We made scatter plots based on whether the posterior mean of RR is greater than 1 and the distribution of factor values to compare the promoting/inhibiting effects under different economic conditions.

Wei, et al., 2022; Tian, Liang, et al., 2018). From a demographic perspective, as shown in Fig. S5 of appendix A, the proportion of HFMD cases by gender and age remains similar to the conclusion provided by the existing study (Guo et al., 2020). HFMD cases in suburban areas account for the smallest proportion of the population but demonstrate the highest incidence, which also suggests that we should strengthen the surveillance of potential exposed populations in suburban areas.

Moreover, it is found that the impact of most meteorological factors on HFMD is temporally associated with the high-incidence season of HFMD. Since human body becomes more prone to sweat in a hot and humid environment, enteroviruses are more likely to attach to the body surface for transmission. At the same time, the increased demand for cool food and water in summer will also lead to a rise in the risk of enterovirus invasion in the external environment. However, when temperature, relative humidity and air pressure rise to a certain high level, the outdoor activities will correspondingly decrease and instead reduce the risk of HFMD, which is different from the conclusions given by research in tropical areas (Jiang, Xu, Lai, & Lin, 2021). Additionally, compared with the north-to-south wind, the east-to-west wind exerts a more

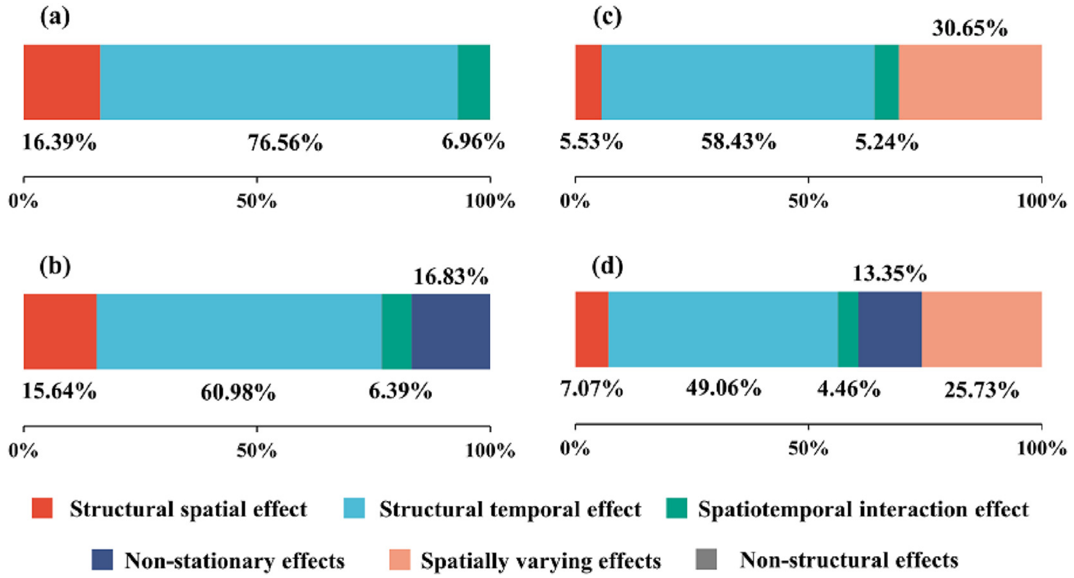

Fig. 7. The proportion of posterior marginal variances of different components included in Bayesian models. (a) Results with only spatiotemporal effects modeled. (b) Results after incorporating non-stationary effects. (c) Results after incorporating spatially varying effects. (d) Results after incorporating non-stationary and spatially varying effects. In addition to changing the included environmental factors with different effects, all the other modules and parameters of the Bayesian spatiotemporal mapping model remain unchanged.

evident impact on HFMD occurrence, possibly owing to the spatial distribution of air passages in urban areas formed by the special long and narrow terrains of Xi'an city (City Situation-Xi'an Municipal People's Government, 2022). In terms of the influence of meteorological fluctuations, the facilitating effect of the increase in temperature on the risk of HFMD is found more significant in the 3-year period, while the inhibitory effect of the increase in precipitation is more obvious in the 5-year period. A previous study in North China pointed out that large fluctuations in environmental conditions may prevent the reproduction and transmission of enteroviruses (Xu et al., 2020), and our results proved this conclusion by focusing on the impact of temperature and precipitation fluctuations on HFMD.

With regard to air pollutants, atmospheric particulate $PM_{2.5}$, PM_{10} and harmful gas NO_2 have a similar inverted U-shaped effects on the risk of HFMD. The concentration of these pollutants becomes higher in winter, which will lead to poor air quality and even haze weather. In this case, residents usually take personal protective measures such as wearing masks and reducing outdoor activities, indirectly resulting in a decline in the risk of enterovirus infection. Likewise, a high concentration of SO_2 will cause the human body feel evidently uncomfortable, which will facilitate taking protective measures with virus defense functions. Different from these aforementioned pollutants, O_3 tends to display a higher concentration in summer. When the concentration of O_3 exceeds a certain threshold, it will induce photochemical smog which can dramatically stimulate human mucous membranes and damage the respiratory system, further increasing the risk of enterovirus invasion. Our analysis of the relationship between air pollutants and HFMD strengthen the conclusion of an existing linear correlation obtained by other scholars (He et al., 2020; Li, Zhu, et al., 2022).

In addition, previous studies always focus the impact of socio-economic factors on HFMD on current local conditions, but different stages of development also need to be considered. Population density can explain part of the spatial pattern of HFMD risk, but its impact on HFMD is not balanced in both time and space. Population density in the suburbs of Xi'an is positively correlated with the risk of HFMD, while that in the core urban area and most rural areas has a negative correlation with HFMD occurrence. Further analysis also revealed that the correlation between population density and HFMD risk is stronger in the high-density stage. However, the population density of the core urban area has always maintained a negative correlation with HFMD risk before and after the segmental fitting, probably because its population has entered a stage of slow growth, when the level of public facilities and health management is gradually catching up with economic development. This result once again proves that rapid urbanization process including population aggregation will relatively reduce the risk of HFMD due to the gradual improvement of public health conditions in the later stage. Furthermore, road density in core urban areas is negatively correlated with HFMD risk, similar to that between GDP and HFMD in the large city (He et al., 2020). In contrast, nightlight in the same area is positively correlated with HFMD, which could be attributed to the fact that places with strong nightlight tend to have more economic activities and frequent crowd contact. Besides, the influence of interventions during the COVID-19 pandemic on the risk of HFMD should not be ignored, as we have discussed the changes in HFMD prevalence patterns after 2020 in the previous study (Shen, Sun, Song, et al., 2022). The sensitivity analysis results of Table S1 in Appendix A show that the association of some environmental factors (e.g., temperature) with the risk of HFMD in Xi'an has changed significantly in 2020. This is mainly because the high incidence season of HFMD in Xi'an has shifted into autumn and winter under the intervention of anti-COVID-19 prevention and control measures (Shen, Sun, Song, et al., 2022). In 2021, with the seasonal peak of HFMD in Xi'an returning to summer (Shen, Sun, Song, et al., 2022), the driving effect of multiple factors also exhibited a trend of towards normal. In order to further explore this phenomenon, we will dedicate to continually collect HFMD data after 2020 in future research.

The contribution of this study are threefold. Firstly, the construction of a Bayesian spatiotemporal mapping model demonstrates the possibility of quantitatively capturing the association between HFMD and its environmental factors by considering various driving effects, providing a methodological framework to not only the epidemiology of HFMD but also other infectious disease research. Secondly, the incorporation of a spatiotemporal perspective to the traditional statistical research can improve the accuracy and reliability of conclusions especially through integrating multiple data sources based on geospatial techniques. It helps found the causes of non-stationary relationships are mainly seasonal variations and threshold effects of meteorological conditions, and spatial variation relationships are mainly influenced by human production activities and lifestyle, as well as the uneven distributions of economic factors. Thirdly, potential advantages of this research can also be found beyond the academic community. It has practical values in supporting prevention and control of HFMD by public health institutions. The general public living in high-altitude regions need to be acknowledged with epidemiological characteristics of HFMC, and an optimized allocation of medical resources in their settlements is of necessity. It is critical to recognize that kindergartens and primary schools in suburbs should be given regular daily disinfection and symptom monitoring to cope with the potential risk of HFMD transmission and outbreak brought about by rapid urbanization. Besides, governments are obligated to release early warning in time during the high-incidence season of HFMD and adjust the information according to the changes occurring in the relationship with meteorological factors.

4.2. Limitations

This study also presents several limitations and opportunities for further epidemiological research of HFMD. Firstly, due to the difficulty in obtaining laboratory-tested samples, we did not take the influence of different enterovirus serotypes into our study. In recent years, the predominant serotype of the HFMD cases in Xi'an has been identified EV-A71, followed by CV-A16. In future research, it is imperative for researchers to consider the impact of enterovirus serotypes on the occurrence of HFMD, as different serotypes exhibit distinct responses to environmental conditions such as temperature and precipitation. Secondly, with respect to our methodologies, the modeling of non-stationary effects and spatially varying effects in this Bayesian model is independent, which may lead to missing some relationships with both spatial and non-spatial variation characteristics. Thirdly, the proportion of children under 5 years old has a significant impact on the incidence rate of HFMD. Unfortunately, we did not obtain population age group data at the township level. In future research, this could be addressed by expanding the study area and geographic scale to incorporate the influence of the proportion of children. In addition, the confirmation of the correlation derived in this study does not necessarily imply a definite causal link, but it can still help monitor and respond to the changes in HFMD risk.

5. Conclusions

To conclude, this study quantitatively explored both non-stationary and spatially varying effects of multiple environmental factors on the occurrence of HFMD, based on a proposed Bayesian spatiotemporal mapping model. These findings will not only support the practical prevention and control of HFMD in potential endemic areas, but also provide a promising model framework that can be extended to investigate outbreak risk of other infectious diseases.

Funding

This work was supported by grants from the National Natural Science Foundation of China (L.S., grant number: 42201448), (K.L., grant number: 82273689); and Natural Science Foundation of Hubei Province (L.S., grant number: 2022CFB610).

Ethics approval and consent to participate

Ethical review and approval was not required for the study on human participants in accordance with the local legislation and institutional requirements. Written informed consent for participation was not required for this study in accordance with the national legislation and the institutional requirements. Written informed consent was not obtained from the individual(s) for the publication of any potentially identifiable images or data included in this article.

Consent for publication

Not applicable.

Data availability

The original research data for this paper can be obtained by sending a request email to the corresponding author(-liukun5959@qq.com).

CRediT authorship contribution statement

Li Shen: Writing – original draft, Methodology, Formal analysis, Data curation. **Minghao Sun:** Writing – original draft, Software, Investigation, Formal analysis, Data curation. **Mengna Wei:** Writing – original draft, Investigation, Formal analysis, Conceptualization. **Qingwu Hu:** Writing – review & editing. **Yao Bai:** Conceptualization. **Zhongjun Shao:** Writing – review & editing, Conceptualization. **Kun Liu:** Writing – review & editing, Conceptualization.

Declaration of competing interest

The authors declare that the research was conducted in the absence of any commercial or financial relationships that could be construed as a potential conflict of interest.

Acknowledgements

The authors were grateful and extended their appreciation to anonymous reviewers whose suggestions helped in the preparation of this paper.

Appendix A. Supplementary data

Supplementary data to this article can be found online at https://doi.org/10.1016/j.idm.2024.02.005.

Abbreviations

CAR	conditional autoregressive
EV-A71	Enterovirus A71
HFMD	hand, foot, and mouth disease
INLA	Integrated nested Laplace approximation
POIs	points of interest
RR	relative risk

References

City Situation-Xi'an Municipal People's Government. (2022). *Local chronicle of Xi'an.* Retrieved from http://www.xa.gov.cn/sq/. (Accessed 5 June 2023).

Du, Z., Lawrence, W. R., Zhang, W., Zhang, D., Yu, S., & Hao, Y. (2018). Bayesian spatiotemporal analysis for association of environmental factors with hand, foot, and mouth disease in guangdong, China. *Scientific Reports, 8*(1), Article 15147. https://doi.org/10.1038/s41598-018-33109-3

Esposito, S., & Principi, N. (2018). Hand, foot and mouth disease: Current knowledge on clinical manifestations, epidemiology, aetiology and prevention. *European Journal of Clinical Microbiology & Infectious Diseases, 37*(3), 391–398. https://doi.org/10.1007/s10096-018-3206-x

Gou, F., Liu, X., Ren, X., Liu, D., Liu, H., Wei, K., et al. (2017). Socio-ecological factors and hand, foot and mouth disease in dry climate regions: A bayesian spatial approach in gansu, China. *International Journal of Biometeorology, 61*(1), 137–147. https://doi.org/10.1007/s00484-016-1197-9

Guo, T., Liu, J., Chen, J., Bai, Y., Long, Y., Chen, B., et al. (2020). Seasonal distribution and meteorological factors associated with hand, foot, and mouth disease among children in xi'an, northwestern China. *The American Journal of Tropical Medicine and Hygiene, 102*(6), 1253–1262. https://doi.org/10.4269/ajtmh.19-0916

He, X., Dong, S., Li, L., Liu, X., Wu, Y., Zhang, Z., et al. (2020). Using a bayesian spatiotemporal model to identify the influencing factors and high-risk areas of hand, foot and mouth disease (HFMD) in shenzhen. *PLoS Neglected Tropical Diseases, 14*(3), Article e0008085. https://doi.org/10.1371/journal.pntd.0008085

Hong, J., Liu, F., Qi, H., Tu, W., Ward, M. P., Ren, M., et al. (2022). Changing epidemiology of hand, foot, and mouth disease in China, 2013–2019: A population-based study. *The Lancet Regional Health - Western Pacific, 20*, Article 100370. https://doi.org/10.1016/j.lanwpc.2021.100370

Hu, X., Jiang, F., & Ni, W. (2018). Floods increase the risks of hand-foot-mouth disease in qingdao, China, 2009-2013: A quantitative analysis. *Disaster Medicine and Public Health Preparedness, 12*(6), 723–729. https://doi.org/10.1017/dmp.2017.154

Jiang, Y., Xu, J., Lai, H., & Lin, H. (2021). Association between meteorological parameters and hand, foot and mouth disease in mainland China: A systematic review and meta-analysis. *Iranian Journal of Public Health*. https://doi.org/10.18502/ijph.v50i9.7046

Lei, H., Zhang, N., Niu, B., Wang, X., Xiao, S., Du, X., et al. (2023). Effect of rapid urbanization in mainland China on the seasonal influenza epidemic: Spatiotemporal analysis of surveillance data from 2010 to 2017. *JMIR Public Health and Surveillance, 9*, Article e41435. https://doi.org/10.2196/41435

Li, C., Zhu, Y., She, K., Jia, Y., Liu, T., Han, C., et al. (2022). Modified effects of air pollutants on the relationship between temperature variability and hand, foot, and mouth disease in zibo city, China. *Environmental Science and Pollution Research, 29*(29), 44573–44581. https://doi.org/10.1007/s11356-022-18817-8

Li, M., Ma, Y., Luo, C., Lv, Q., Liu, Y., Zhang, T., et al. (2022). Modification effects of socioeconomic factors on associations between air pollutants and hand, foot, and mouth disease: A multicity time-series study based on heavily polluted areas in the basin area of sichuan province, China. *PLoS Neglected Tropical Diseases, 16*(11), Article e0010896. https://doi.org/10.1371/journal.pntd.0010896

Muñoz, J. (2019). In *ERA5-Land monthly averaged data from 1950 to present. Copernicus Climate change Service (C3S) climate data store (CDS)*. https://doi.org/10.24381/cds.68d2bb30

Shaanxi Provincial Public Data Platform. (2022). List of health and medical institutions in Shaanxi province. Retrieved from http://www.sndata.gov.cn. (Accessed 5 June 2023).

Shen, L., Sun, M., Song, S., Hu, Q., Wang, N., Ou, G., et al. (2022). The impact of anti-COVID-19 nonpharmaceutical interventions on hand, foot, and mouth disease - a spatiotemporal perspective in xi'an, northwestern China. *Journal of Medical Virology, 94*(7), 3121–3132. https://doi.org/10.1002/jmv.27715

Shen, L., Sun, M., Wei, X., Bai, Y., Hu, Q., Song, S., et al. (2022). Spatiotemporal association of rapid urbanization and water-body distribution on hemorrhagic fever with renal syndrome: A case study in the city of xi'an, China. *PLoS Neglected Tropical Diseases, 16*(1), Article e0010094. https://doi.org/10.1371/journal.pntd.0010094

Simonart, T., Lam Hoai, X.-L., & De Maertelaer, V. (2022). Worldwide evolution of vaccinable and nonvaccinable viral skin infections: Google trends analysis. *JMIR Dermatology, 5*(4), Article e35034. https://doi.org/10.2196/35034

Tian, H., Hu, S., Cazelles, B., Chowell, G., Gao, L., Laine, M., et al. (2018). Urbanization prolongs hantavirus epidemics in cities. *Proceedings of the National Academy of Sciences, 115*(18), 4707–4712. https://doi.org/10.1073/pnas.1712767115

Tian, L., Liang, F., Xu, M., Jia, L., Pan, X., & Clements, A. C. A. (2018). Spatio-temporal analysis of the relationship between meteorological factors and hand-foot-mouth disease in beijing, China. *BMC Infectious Diseases, 18*(1), 158. https://doi.org/10.1186/s12879-018-3071-3

Wang, Y., Lai, Y., Du, Z., Zhang, W., Feng, C., Li, R., et al. (2019). Spatiotemporal distribution of hand, foot, and mouth disease in guangdong province, China and potential predictors, 2009-2012. *International Journal of Environmental Research and Public Health, 16*(7), 1191. https://doi.org/10.3390/ijerph16071191

Wei, J., Li, Z., Lyapustin, A., Sun, L., Peng, Y., Xue, W., et al. (2021). Reconstructing 1-km-resolution high-quality PM2.5 data records from 2000 to 2018 in China: Spatiotemporal variations and policy implications. *Remote Sensing of Environment, 252*, Article 112136. https://doi.org/10.1016/j.rse.2020.112136

Wei, J., Li, Z., Wang, J., Li, C., Gupta, P., & Cribb, M. (2023). Ground-level gaseous pollutants (NO_2, SO_2, and CO) in China: Daily seamless mapping and spatiotemporal variations. *Atmospheric Chemistry and Physics, 23*(2), 1511–1532. https://doi.org/10.5194/acp-23-1511-2023

WorldPop. (2022). *Individual countries 2000-2020 UN adjusted dataset*. Retrieved from https://hub.worldpop.org/geodata/listing?id=29. (Accessed 5 June 2023).

Xi'an Municipal People's Government. (2022). Xi'an "13th five-year plan" three-year action program for relocation of poverty alleviation and poverty reduction. Retrieved from http://www.xa.gov.cn/gk/zcfg/szfbgtwj/5d495b36f99d6572b76fc465.html. (Accessed 5 June 2023).

Xu, C., Zhang, X., Wang, L., Zhou, Y., Xiao, G., & Liao, J. (2020). Effects of temperature fluctuations on spatial-temporal transmission of hand, foot, and mouth disease. *Scientific Reports, 10*(1), 2541. https://doi.org/10.1038/s41598-020-59265-z

Yang, J., & Huang, X. (2021). The 30 m annual land cover dataset and its dynamics in China from 1990 to 2019. *Earth System Science Data, 13*(8), 3907–3925. https://doi.org/10.5194/essd-13-3907-2021

Zhang, L., Ren, Z., Chen, B., Gong, P., Fu, H., & Xu, B. (2021). In *A prolonged artificial nighttime-light dataset of China (1984-2020). A big earth data platform for three Poles*, 10.11888.

Zhang, X., Xu, C., & Xiao, G. (2020). Spatial heterogeneity of the association between temperature and hand, foot, and mouth disease risk in metropolitan and other areas. *Science of the Total Environment, 713*, Article 136623. https://doi.org/10.1016/j.scitotenv.2020.136623

Zhu, H., Chen, S., Liang, R., Feng, Y., Joldosh, A., Xie, Z., et al. (2023). Study of the influence of meteorological factors on HFMD and prediction based on the LSTM algorithm in fuzhou, China. *BMC Infectious Diseases, 23*(1), 299. https://doi.org/10.1186/s12879-023-08184-1

Zhu, N., Zhou, T., Yang, G., Li, X., Wang, S., & Zhang, Y. (2021). Spatial and temporal distribution and epidemic intensity of hand, foot and mouth disease in Shaanxi Province from 2009 to 2018. *Chinese Journal of Disease Control & Prevention, 25*(1), 54–59. https://doi.org/10.16462/j.cnki.zhjbkz.2021.01.011